Scientific paper

Halogenido Analogues of Structuraly Diverse Complexes With 3-Hydroxypyridine

Primož Šegedin,[1]* Urška Dolničar,[1] Mirzet Čuskić,[1] Zvonko Jagličić,[2] Amalija Golobič[1] and Bojan Kozlevčar[1]

[1]*Faculty of Chemistry and Chemical Technology, University of Ljubljana, 1000 Ljubljana, Slovenia*

[2]*Institute of Mathematics, Physics and Mechanics & Faculty of Civil and Geodetic Engineering, University of Ljubljana, 1000 Ljubljana, Slovenia*

** Corresponding author: E-mail: primoz.segedin@fkkt.uni-lj.si*
Tel.: 00 386 1 2419 122; Fax: 00 386 1 2419 220

Received: 12-05-2008

Dedicated to the memory of Professor Ljubo Golič

Abstract

Two types of bromido and chlorido complexes with 3-hydroxypyridine (3-pyOH), namely, $[CuX_2(3\text{-pyOH})_4]$ (**1**, **2**) type A, and $[Cu(\mu\text{-}X)_2(3\text{-pyOH})_2]_n$ (**3**, **4**) type B (X = Br, Cl) were prepared. The X-ray single crystal structure determination of the mononuclear $[CuBr_2(3\text{-pyOH})_4]$ **1** reveals octahedral coordination with four nitrogen atoms of 3-pyOH molecules in the equatorial plane and two bromido anions in the axial positions. A structure of the type A chlorido analogue $[CuCl_2(3\text{-pyOH})_4]$ **2** was determined by a combination of the powder and the single crystal diffraction data. The molecular structure of the type B bromido complex $[Cu(\mu\text{-}Br)_2(3\text{-pyOH})_2]_n$ **3** was also determined from the single crystal XRD data. Herein, infinite linear chains of *catena*-di-μ-bromidobis(3-pyOH)copper(II) are present. A comparison of the powder diffraction data of compounds $[Cu(\mu\text{-}X)_2(3\text{-pyOH})_2]_n$ **3** and **4**, together with their results of IR, UV-Vis and magnetic methods show, that both compounds **3** and **4** can be assigned as the type B, due to their probably very similar molecular structure. The magnetic susceptibility of the type A mononuclear complexes shows a paramagnetic behaviour in the range 2–300 K with a constant $\chi_M \cdot T$ value. On the other hand, a broad maximum of the curve χ_M versus T below 50 K for the type B polynuclear complexes, reveals the antiferromagnetic interaction between the copper(II) $S = ½$ magnetic moments. These data were fitted by the Bonner-Fisher curve (1D Heisenberg antiferromagnet) giving J –17 cm^{-1} (**3**), –10 cm^{-1} (**4**). The paramagnetic behaviour of the polynuclear complexes **3**, **4**, noticed from the room temperature EPR spectra, is in agreement with the spin of copper(II), and the rhombic distortion of the spin tensor close to the axial symmetry.

Keywords: Copper(II), halogenide, 3-hydroxypyridine, polymer, monomer, antiferromagnet

1. Introduction

Structural and magnetic properties of the binuclear and the polynuclear metal complexes containing monoatomic bridges are of considerable interest from standpoint of inorganic and bioinorganic chemistry. Many of these complexes are relevant as models for the active sites of biomolecules, and also due to their magnetic properties. Copper(II) complexes with the monoatomic bridges have been extensively studied, especially those containing chlorido and bromido bridging ligands, to develop a correlation between the molecular structure and the magnetic behaviour.[1–7] The antiferromagnetic superexchange interactions between the adjacent copper(II) ions were observed in linear-chain $[Cu(\mu\text{-}X)_2L_2]_n$ type of compounds (X = Cl, Br; L = substituted-pyridine or azole). An influence of the structural factors and the type of a ligand, on the magnitude of the magnetic interaction, were studied for these complexes.[8]

Herein, the structural and magnetic analyses of the linear chain complexes $[Cu(\mu\text{-}Br)_2(3\text{-pyOH})_2]_n$ (3-pyOH = 3-hydroxypyridine) and $[Cu(\mu\text{-}Cl)_2(3\text{-pyOH})_2]_n$ are presented. These two complexes are correlated with the mononuclear $[CuBr_2(3\text{-pyOH})_4]$ and $[CuCl_2(3\text{-pyOH})_4]$ analogues.

2. Experimental

2. 1. Materials and Synthesis

All reagents were obtained commercially and were used without further purification.

$[CuBr_2(3\text{-pyOH})_4]$ **1**

3-pyOH (1.15 g, 12 mmol) was dissolved in a mixture of acetonitrile, absolute ethanol (7 + 5 mL), and $CuBr_2$ (0.34 g, 1.5 mmol) was added. Diethyl ether (20 mL) was added to the obtained solution, and left at room temperature for 24 h. Blue crystals of **1** were filtered off and dried over KOH for 24 h. Average yield 75%. Anal. calcd for $C_{20}H_{20}Br_2CuN_4O_4$: C 39.9, H 3.35, N 9.31, Cu 10.6, Br 26.7. Found: C 39.8, H 3.40, N 9.26, Cu 10.5, Br 26.4. IR ν 3130s, 1620w, 1596s, 1582vs, 1482w, 1471m, 1440vs, 1350w, 1290s, 1272vs, 1238m cm^{-1}. UV/Vis λ_{max} 250sh, 310, 380sh, 590 nm. EPR $g_{\|}$ 2.160(5), $g_{\perp}$ 2.078(5).

$[CuCl_2(3\text{-pyOH})_4]$ **2**

3-pyOH (0.76 g, 8.0 mmol) was dissolved in 5 mL of absolute ethanol. This solution was added dropwise during stirring to the solution of $CuCl_2 \cdot 2H_2O$ (0.17 g, 1.0 mmol) in 5 mL of acidified water (one drop of formic acid). A small amount of a solid residue was filtered off after 15 min. The filtrate was left at 6 °C for four days, when dark blue crystals of **2** were filtered off. They were dried on air for 15 min and over KOH for 24 h. Average yield 53%. Anal. calcd for $C_{20}H_{20}Cl_2CuN_4O_4$: C 46.7, H 3.92, N 10.9, Cu 12.4, Cl 13.8. Found: C 47.2, H 4.03, N 11.0, Cu 12.2, Cl 13.8. IR ν 3100vs, 1620m, 1598m, 1580vs, 1482s, 1446s, 1362m, 1292vs, 1280s, 1242m cm^{-1}. UV/Vis λ_{max} 250sh, 300, 380sh, 590 nm. EPR g_1 2.169(5), g_2 2.107(5), g_3 2.064(5).

$[Cu(\mu\text{-}Br)_2(3\text{-pyOH})_2]_n$ **3**

3-pyOH (0.30 g, 3.2 mmol) was dissolved in a mixture of acetonitrile, absolute ethanol (3 + 2 mL), and the obtained solution was added to the solution of $CuBr_2$ (0.34 g, 1.5 mmol) in acetonitrile (15 mL). The final solution was left at 6 °C for a day. Green crystals of **3** were filtered off, dried on air for 15 min and over KOH for 24 h. Average yield 79%. Anal. calcd for $C_{10}H_{10}Br_2CuN_2O_2$: C 29.0, H 2.44, N 6.77, Cu 15.4, Br 38.6. Found: C 29.2, H 2.41, N 6.59, Cu 15.3, Br 39.2. IR ν 3310s, 1620w, 1586vs, 1484s, 1464m, 1355w, 1288s, 1273m, 1209m cm^{-1}. UV/Vis λ_{max} 235sh, 300, 370, 460sh, 645 nm. EPR g_{av} 2.104(5).

$[Cu(\mu\text{-}Cl)_2(3\text{-pyOH})_2]_n$ **4**

3-pyOH (0.38 g, 4.0 mmol) was dissolved in methanol (45 mL) and $CuCl_2 \cdot 2H_2O$ (0.34 g, 2.0 mmol) was added. The obtained suspension was heated till boiling and then filtered. The filtrate was slowly cooled down to the room temperature and then left at 6 °C for a day. The green-blue crystals of **4** were filtered off, dried on air for 15 min and over KOH for 24 h. Average yield 65%. Anal. calcd for $C_{10}H_{10}Cl_2CuN_2O_2$: C 37.0, H 3.10, N 8.63; Cu 19.6, Cl 21.8. Found: C 37.1, H 3.23, N 8.53 Cu 19.4 Cl 22.0. IR ν 3295vs, 1619m, 1587vs, 1483s, 1462m, 1357w, 1290s, 1278m, 1213s cm^{-1}. UV/Vis λ_{max} 250sh, 300, 400sh, 640 nm. EPR g_1 2.226(5), g_2 2.086(5), g_3 2.059(5).

2. 2. Physical Measurements

C,H,N analyses were performed with a Perkin-Elmer 2400 CHN Elemental Analyzer. Metal analysis was carried out electrogravimetrically with Pt electrodes, while halogenido analysis with potentiometric titration using $AgNO_3$. Vibrational spectra of the KBr pellets were recorded on a Perkin-Elmer 1720-X FT-IR spectrometer. Electronic spectra were recorded as nujol mulls with a Perkin-Elmer Lambda 19 UV/Vis/NIR spectrometer. X-band powder EPR spectra were recorded at room temperature on a Bruker ESP-300 electron spin resonance spectrometer. The g values were calculated by the equation $E = h\nu = g\beta_e B$. The magnetic susceptibility data between 2 and 300 K of powdered samples were obtained with a Quantum Design SQUID magnetometer in H 1000 Oe. They were corrected for the sample holder and the diamagnetic response of the compounds estimated from the Pascal's constants.[10] Powder XRD data were obtained with a PANalytical X'Pert PRO MPD diffractometer for **1** and **3** and with an Enraf Nonius Guinier camera for **2** and **4**, both with Cu K_α radiation.

2. 2. The Molecular Structure Determination

The single crystal diffraction data of compounds **1** and **3** were collected with a Nonius Kappa CCD diffracto-

Table 1: d-spacings (Å) with their relative intensities I/I_0 in parentheses for the powder XRD data of **1**–**4**.[9]

1	8.05	7.80		6.10	5.97	5.61	4.64	4.16	4.06	4.01	3.90	3.71
	10	2		1	<1	2	3	5	3	2	3	3
2	8.03	7.77	6.48	6.05	5.92	5.56	4.61	4.12		3.97	3.84	3.65
	10	8	1	2	1	9	7	4		3	1	5
3	9.01	7.76	6.22	4.92	4.30	4.18	3.99	3.92	3.88	3.83	3.50	3.35
	2	10	<1	2	2	1	2	<1	1	<1	4	1
4	8.66	8.01	6.23	4.87			3.99	3.91	3.75	3.68	3.54	3.45
	5	10	3	7			4	2	8	9	4	1

meter using a graphite monochromated Mo K_α radiation. They were processed using the DENZO-SMN program.[11] Both structures were solved by direct methods using SIR97.[12] The position of the hydroxy H3 atom in **3** was placed on the line between O3 and Br (O3–H3 = 0.96 Å), while the positions of all the other hydrogen atoms in **1** and **3** were obtained from the difference Fourier map. Full-matrix least-squares refinement on *F* magnitudes was employed with the anisotropic displacement factors for all non-hydrogen atoms using Xtal3.6.[13] The parameters of hydrogen atoms were not refined. 1065 and 2139 reflections ("less than" reflections $F_c > F_o$) with 79 and 141 parameters were used in the final cycle of the refinement for **1** and **3**, respectively. The resulting crystal data and details concerning data collection and refinement for **1** and **3** are quoted in Table 2.

The molecular structure of compound **2** was determined differently as for **1** and **3**, by using a combination of the single crystal and the powder diffraction data. The single crystal data for **2** were collected and processed as described for **1** and **3**. However, three attempts with crystals from different samples, that all resulted in the same chemically reasonable structural model, were unfortunately not refined successfully ($R > 0.10$, a large and chemically unreasonable residual maximum in the difference Fourier map). Therefore, the powder diffraction data on PANalytical X'Pert powder diffractometer in 5–100° 2Θ range were collected. The Rietveld refinement (using TOPAS program)[14] of the questionable "single" crystal structural model was successful. 6 background parameters, the scale factor, the zero error parameter, and three parameters describing the crystallite size (one for the strain and two for the preferred orientation of crystallites) were refined. During the refinement of 53 structural parameters (3 cell parameters, 46 coordinates and 4 isotropic

Table 2. Relevant crystal data and data collection summary for **1** and **3**.

Compound	**1**	**3**
Formula	$C_{20}H_{20}Br_2CuN_4O_4$	$C_{10}H_{10}Br_2CuN_2O_2$
Formula relative weight	603.75	413.55
Crystal system	orthorhombic	monoclinic
Space group	*Pcca*	$P2_1/n$ (no.14)
a (Å)	16.2067(3)	4.0475(2)
b (Å)	7.7849(1)	18.0007(8)
c (Å)	18.5079(3)	8.7799(4)
β (°)	90	101.778(2)
V (Å^3)	2335.10(6)	626.22(5)
Z	4	2
D_x (g/cm^3)	1.717	2.193
μ (mm^{-1})	4.391	8.114
T (K)	293	293
Crystal colour	blue	green
Crystal shape	prism	needle
Crystal size (mm)	0.25 × 0.20 × 0.15	0.30 × 0.08 × 0.01
Θ max (°)	26.0	25.3
R_{int}	0.033	0.061
Threshold	$F^2>2.0\sigma(F^2)$	$F^2>2.0\sigma(F^2)$
Total (integrated) data	31238	7346
Independent data	2269	1132
Observed data	1937	967
Contributing data	2139	1065
Refined parameters	141	79
R	0.038	0.065
R_w	0.027	0.051
$\Delta\rho_{min,max}$ (eÅ^{-3})	–0.514, 0.671	–1.528, 1.423*

$R = \Sigma(||F_o|-|F_c||)\Sigma|F_o|$; $Rw = \Sigma(w(|F_o|-|F_c|))/\Sigma(w|F_o|)$; * satelite peaks of Br

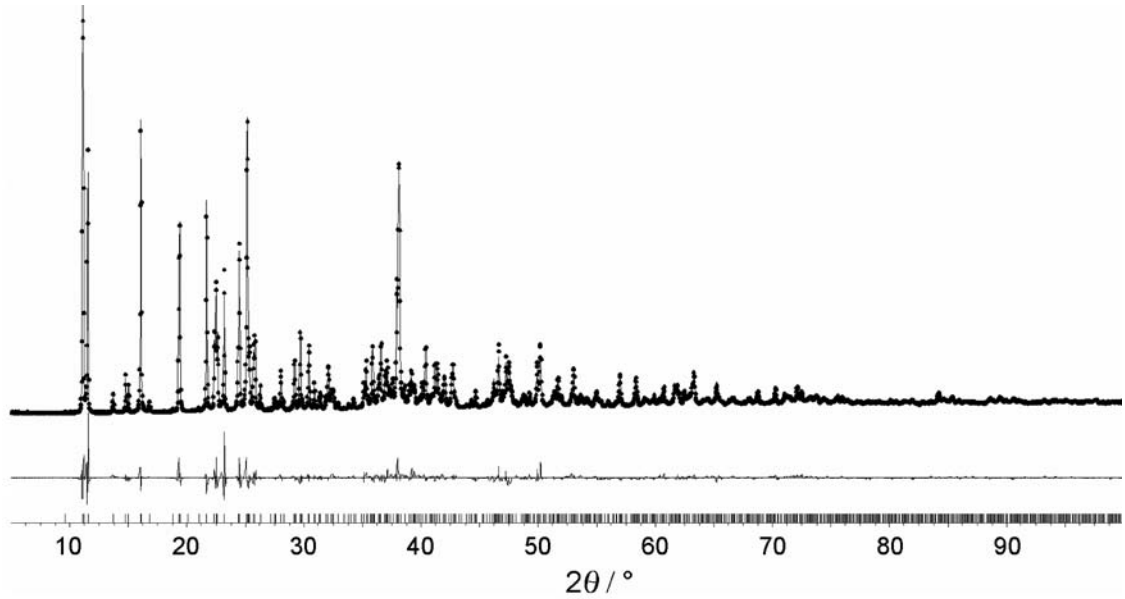

Figure 1. The powder XRD difrractogram of compound **2** (◦) with the calculated data (solid line). A difference between both data is shown as the lower solid line. Vertical bars below denote the positions of reflections.

Table 3. Relevant crystal data and data collection summary for **2**.

Compound	**2**
Formula	$C_{20}H_{20}Cl_2CuN_4O_4$
Formula relative weight	514.86
Crystal system	orthorhombic
Space group	*Pcca*
a (Å)	15.8142(4)
b (Å)	7.6628(2)
c (Å)	18.3865(4)
V (Å^3)	2228.10(9)
Z	4
D_x (g/cm^3)	1.535
μ (mm^{-1})	3.890
T (K)	293
Crystal colour	blue
Diffractometer	Panalytical X'Pert
Radiation type	Cu K_1
Wavelength (Å)	1.5406
$2\Theta_{MIN, MAX}$ (°)	5-100
Step width (°)	0.033
Time per step (s)	500
Antiscatter slit (mm)	10
Musk (mm)	10
Detector	Full range
No. of profile parameters	13
No. of structural parameters	53
No. of restraints	14
R_p	0.054
R_{wp}	0.078

$R_p = ((\Sigma|Y_{o,m} - Y_{c,m}|)/(\Sigma Y_{o,m}))^{½}$;
$R_{wp} = ((\Sigma w_m(Y_{o,m} - Y_{c,m})^2)/(\Sigma w_m(Y_{o,m})^2))^{½}$; $Y_{o,m}$ and $Y_{c,m}$ are the observed and the calculated data, respectively, at data point m.[14]

displacement parameters, constrained to be equal for each type of atoms), 14 restraints for the 3-pyOH bond lengths were applied. The final data show a good agreement between the calculated and the observed diffraction patterns (R_p 0.054, Figure 1), without any questionable residual electron density. The final crystal data and the details concerning powder data collection and the Rietveld refinement are quoted in Table 3. A correctness of the thus determined crystal structure of **2** is additionally proved by the single crystal structure determination of **1**, that was determined straightforward and reveals isostructurallity to **2** (Tables 2–4). The crystallographic data for **1**–**3** have been deposited with the Cambridge Crystallographic Data Center as supplementary material with the deposition numbers: CCDC 687274-687276, respectively. Copies of the data can be obtained, free of charge via http://www.ccdc.cam.ac.uk/const/retrieving.html.

3. Results and Discussion

3. 1. Description of the Crystal Structures

The molecular structure of $[CuBr_2(3\text{-pyOH})_4]$ **1** (Figure 2) is formed by four 3-pyOH molecules cation laying on two-fold axis, via bonded to the central copper(II) cation via nitrogen atoms (Cu–N = 2.046(3), 2.055(3) Å). The coordination octahedron around copper is completed by two bromido anions (Cu–Br = 3.023(1) Å) situated on the elongated Jahn-Teller axis Br–Cu–Br. The structure is stabilized by hydrogen bonding O–H···Br (3.136(3) Å, 152; 3.138(3) Å, 178). A similar coordination mode with four *trans* oriented pyridine ligands, and the orthorhombic system as in **1**, is found in $[CuBr_2py_4] \cdot 2py$. This compound is stable as a pyridine solvate, and a solvate evaporation at room temperature leads to its decomposition resulting in polynuclear $CuBr_2py_2$.[15]

Though the crystal structure determination of $[CuCl_2(3\text{-pyOH})_4]$ **2** took place by different route as for **1** (see the experimental section), its molecular structure is found to be analogous to that of **1** (Cu–N 2.089(14), 2.095(14), Cu–Cl 2.839(5) Å; O–H···Cl 2.963(11), 3.012(10) Å, 167, 157°; Table 4). Additionally, the reported cobalt and nickel complexes $[MCl_2(3\text{-pyOH})_4]$ are also isostructural to **2**.[16,17] Both copper complexes **1** and **2** thus belong to the same type A of halogenido/3-pyOH complexes. These mononuclear complex molecules assume a propeller-like conformation. Some related complexes with general formula $[CuX_2L_4]$ are described.[18,19]

The compound $[Cu(\mu\text{-}Br)_2(3\text{-pyOH})_2]_n$ **3** crystallizes in the monoclinic $P2_1/n$ space group with the copper(II) situated at the inversion centre. Copper(II) ion is coordinated by two bromido anions (2.4457(6) Å) and two nitrogen atoms of 3-pyOH (2.018(6) Å), all forming the basal plane of the elongated octahedron (Figure 3). These units are stacked at a distance of 4.0475(2) Å (Cu–Cu') giving 1D structure of infinite chains (*catena*-di-μ-bromidobis(3-pyOH)copper(II) type), as the bromido anions are serving as bridges. On one side, the bromi-

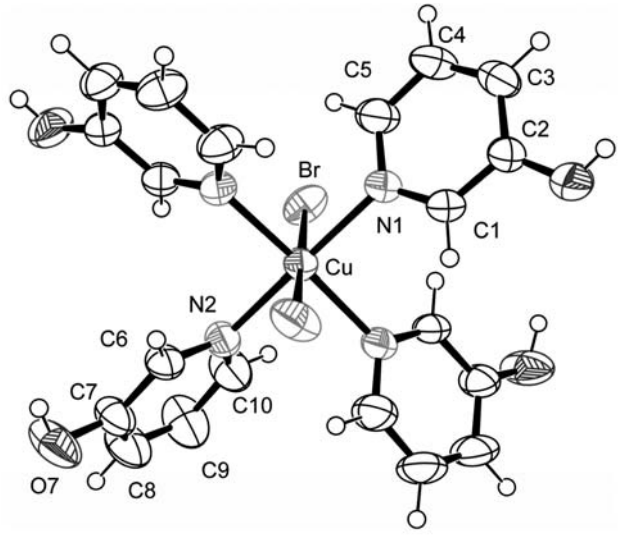

Figure 2. A drawing of the mononuclear complex $[CuBr_2(3\text{-pyOH})_4]$ **1**.[20,21]

Table 4. Coordination bond lengths (Å), and hydrogen bond parameters [distances (Å), angles (°)] in **1–3.**

1					
Cu–Br	3.0229(5)	Cu–N1	2.046(3)	Cu–N2	2.055(3)
D–H···A	D···A	D–H···A	D–H···A	D···A	D–H···A
O2–H2···Br^{i}	3.136(3)	152	O7–H7Br^{ii}	3.138(3)	178
2					
Cu–Cl	2.839(5)	Cu–N1	2.089(14)	Cu–N2	2.095(14)
D–H···A	D···A	D–H···A	D–H···A	D···A	D–H···A
O2–H2···Cl^{iii}	2.963(11)	167	O7–H7···Cl^{II}	3.012(10)	157
3					
Cu–Br	2.4457(6)	Cu–N	2.018(6)	Cu^{iv}–Br	3.2843(7)
D–H···A	D···A	D–H···A	D–H···A	D···A	D–H···A
O–H3···Br^{v}	3.265(6)	180*			

Symmetry operations: ^{i} ½+*x*, *y*, 1–*z*; ^{ii} *x*, –1+*y*, *z*; ^{iii} 1–*x*,1–*y*, 1–*z*; ^{iv} –1+*x*, *y*, *z* ; ^{v} ½–*x*, –½+*y*, ½–*z*; * see the experimental section

do anion is a part of the basal octahedral plane (2.4457(6) Å), while on the other side it occupies the axial position of the adjacent basal octahedral plane (3.2843(7) Å), forming the Jahn-Teller Br–Cu–Br' axis (Figure 3, Table 4) in the elongated coordination octahedron. The structure is stabilized by the O–H···Br (3.265(6) Å, 180°) H-bonds (Table 4) and the pyridine rings π stacking (centroid-centroid distance 4.0475(2) Å, mean interplanar separation 3.647 Å). The halogenido chain-like structural type is found also in some other complexes.[8,22–27] The 3-pyOH molecules are additionally found in different polynuclear copper(II) complexes as terminal or as bridging ligands.[28,29] The XRD powder pattern of $[Cu(\mu\text{-}Cl)_2(3\text{-}pyOH)_2]_n$ **4** shows similarities to that of **3** (Table 1), though not unambiguous as seen for the mononuclear bromido and chlorido analogues **1** and **2** (type A). Nevertheless, the polynuclear complexes **3** and **4** may be assigned as type B.

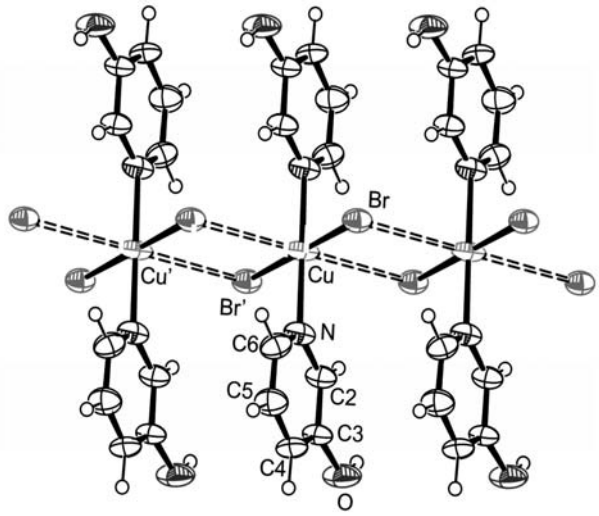

Figure 3. A view on a chain in the molecular structure of $[Cu(\mu\text{-}Br)_2(3\text{-}pyOH)_2]_n$ **3**.[20,21]

3. 2. Spectroscopy and Magnetic Susceptibility

Though the polymeric complexes (type B) are suggested to be isostructural, they show significantly different room temperature EPR spectra. A spectrum of the bromido complex **3** shows one broad isotropic-like signal with $g_{av} = 2.104(5)$, while for the chlorido complex **4** three signals of the rhombically distorted axial symmetry (g_1 2.226(5), g_2 2.086(5), g_3 2,059(5)) are observed. The spectrum with $g_1 >> g_2 > g_3$ is in agreement with the suggested elongated axial coordination sphere in **4**. The EPR spectrum of the mononuclear bromido complex **1** shows poorly resolved axial symmetry signals with $g_{\|}$ 2.160(5) and $g_{\perp}$ 2.078(5). On the other hand, the signals in the EPR spectrum of the chlorido mononuclear type A analogue **2** are slightly better resolved showing g_1 2.169(5), g_2 2.107(5), g_3 2.064(5), though the rhombic symmetry signals are not very clearcut.

The magnetic susceptibility measurements (Figure 4) show almost identical behaviour of both herein described halogenido pairs of compounds **1**, **2** (type A) and **3**, **4** (type B). The mononuclear **1** and **2** are paramagnetic with constant $\chi_M T$ in the range 2–300 K, while the polynuclear **3** and **4** show a significant antiferromagnetic interaction as seen in the χ_M versus T curve with a maximum at 25 K. The experimental data for the type B complexes were fitted by the Bonner-Fischer curve (Equation 1)[10] for the 1D chain-like structures giving **3**: $J = -17$ cm^{-1}, $g = 2.16$; **4**: $J = -10$ cm^{-1}, $g = 2.09$. Larger magnetic exchange interaction $|J|$ for the bromido bridged complex than for the chlorido analogue, is suggested to be due to an easier bromido anion magnetic-orbital contact with copper(II) cation than analogous contact of the chlorido anion. These halogenido bridges are providing the superexchange pathway Cu–X–Cu.[2] Interestingly, the bromido and the chlorido complexes $[Cu(\mu\text{-}X)_2$ (dmamhp)] (X = Br, Cl; dmamhp = 2-dimethylaminomethyl-3-hydroxypyridine), as well as $[Cu(\mu\text{-}X)_2(tz)_2]_n$ (tz = thiazole) showing the antiferromag-

netic interaction with J(Br) < J(Cl) reveal the same relation at the EPR spectra showing only one g_{av} signal for the bromido complex, while much better resolved axial symmetry spectra for the chlorido complex,[2,26] as found for **3** and **4**.

$$\chi_M = \frac{N g^2 \beta^2}{kT} \frac{0.25 + 0.14995\, x + 0.30094\, x^2}{1 + 1.9862\, x + 0.68854\, x^2 + 6.0626\, x^3};\ x = |J|/kT \quad (1)$$

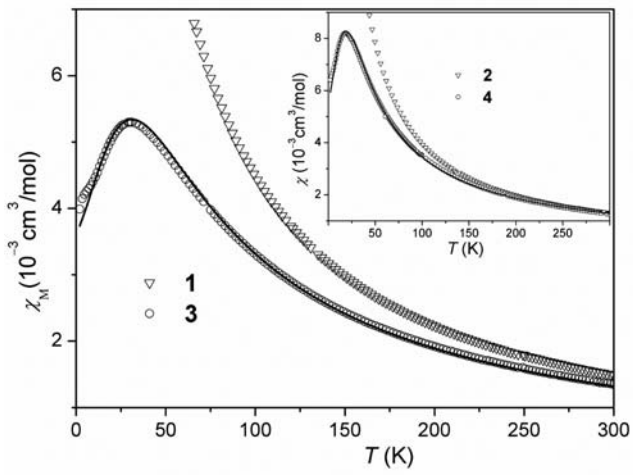

Figure 4: The magnetic susceptibility of the bromido complexes **1** (▽) and **3** (○) and the chlorido complexes **2** (▽) and **4** (○) (inset) as graphs χ_M vs. T. The fitting for the polynuclear (type B) complexes is shown as the solid lines. Parameters are **3**: J = –17 cm^{-1}, g = 2.16; **4**: J = –10 cm^{-1}, g = 2.09.

The IR spectra of all herein described complexes **1–4** are very similar as expected for the complexes with the same or very similar ligands. Some smaller differences are noticed between the spectra of types A and B, especially in the region where the O–H bonds stretching vibrations are expected. Namely, a signal at 3100 cm^{-1} is found in the spectra of the mononuclear (type A) complexes, while at 3300 cm^{-1} in the spectra for the polymeric (type B) complexes. This difference is ascribed to stronger H-bonding contacts O–H···X (thus weaker O–H bond; see Table 4) for the type A complexes (*e. g.* **1**: 3.14 Å, 152–178°), than for the type B complexes (*e. g.* **3**: 3.27 Å, 180°). An analogy between the compounds of the types A and B is clearly visible also in the UV-Vis spectra (see the experimental section).

4. Conclusions

Four halogenido copper(II) complexes with 3-hydroxypyridine (3-pyOH) were synthesized. The single crystal structure determination of both bromido compounds reveals two types of molecular structures, namely, mononuclear in [$CuBr_2$(3-pyOH)$_4$] **1** and polynuclear in [Cu(μ-Br)$_2$(3-pyOH)$_2$]$_n$ **3**. A structure determination of [$CuCl_2$(3-pyOH)$_4$] **2** by a combination of the single crystal and the powder diffraction data shows isostructurality of **2** to **1**, thus both presenting type A. The powder pattern analysis of all four complexes **1**-**4**, together with IR and UV-Vis spectroscopy data clearly suggests strong structural similarity between **1** and **2** (type A), as well as between **3** and **4** (type B). This was additionally confirmed by the magnetic susceptibility data showing similar shapes of the $\chi_M(T)$ curves for **1**, **2** (A) and **3**, **4** (B) pairs (types). The antiferromagnetic interaction found for both polymeric complexes was analyzed with the 1D Bonner-Fisher equation, while the mononuclear type A complexes show expected paramagnetic behavior. A clear resolving of the rhombically distorted axial symmetry EPR signals for the chlorido complex **4**, and only a broad isotropic-like signal for the bromido analogue **3**, may well be related with the stronger antiferromagnetic interaction for the bromido complex **3** than for the chlorido complex **4**. Though bromido (**1**, **3**) and chlorido (**2**, **4**) complexes on first view seem almost complete analogues, certain differences are found especially for their magnetic properties. They probably originate in the magnetic orbital contacts that are related to a different nature of the chlorido and bromido anions.

5. Acknowledgements

We thank Dr. Marjeta Šentjurc, EPR center, 'Jožef Stefan' Institute, Ljubljana, for the EPR data. The financial support of MVZT P1-0175-103, Republic of Slovenia, is gratefully acknowledged.

6. References

1. B. Zurowska, J. Mrozinski, Z. Ciunik, *Polyhedron* **2007**, *26*, 3085–3091.
2. Y. M. Lee, H. W. Lee, Y. I. Kim, *Polyhedron* **2005**, *24*, 377–382.
3. B. Zurowska, K. Slepokura, *Inorg. Chim. Acta* **2008**, *361*, 1213–1221.
4. H. Grove, J. Sletten, M. Julve, F. Lloret, *J. Chem. Soc., Dalton Trans.* **2001**, 2487–2493.
5. E. Colacio, M. Ghazi, R. Kivekas, J. M. Moreno, *Inorg. Chem.* **2000**, *39*, 2882–2890.
6. M. Rodriguez, A. Llobet, M. Corbella, *Polyhedron* **2000**, *19*, 2483–2491.
7. K. S. Burger, P. Chaudhuri, K. Wieghardt, *Inorg. Chem.* **1996**, *35*, 2704–2707.
8. J. A. C. van Ooijen, J. Reedijk, E. J. Sonneveld, J. W. Visser, *Transit. Met. Chem.* **1979**, *4*, 305–307.
9. X'Pert HighScore, PANalitical B. V., Almelo, The Netherlands, **2005**.
10. O. Kahn, *Molecular Magnetism*, VCH, **1993**.

11. Z. Otwinowski, W. Minor, *Methods in Enzymology*, Vol. 276, M*acromolecular Crystallography*, Part A (Eds.: C. W. Carter Jr., R. M. Sweet), Academic Press, **1997**, pp. 307–326.
12. A. Altomare, M. C. Burla, M. Camalli, G. Cascarano, C. Giacovazzo, A. Guagliardi, A. G. G. Moliterni, G. Polidori, S. R., *J. Appl. Crystallogr.* **1999**, *32*, 115–119.
13. S. R. Hall, D. J. du Boulay, R. Olthof-Hazekamp (Eds.), The XTAL3.6 System, University of Western Australia, Lamb, Perth, Australia, **1999**.
14. Bruker AXS, Topas, General profile and structure analysis software for powder diffraction data, Karlsruhe, Germany, **2003**.
15. M. Selkti, C. C. Ling, A. Navaza, *J. Incl. Phenom. Macro.* **1994**, *17*, 127–135.
16. S. Gao, X. F. Zhang, L. H. Huo, Z. Z. Lu, H. Zhao, J. G. Zhao, *Acta Crystallogr. E* **2004**, *60*, M1128-M1130.
17. X. F. Zhang, S. Gao, L. H. Huo, Z. Z. Lu, H. Zhao, *Acta Crystallogr. E* **2004**, *60*, M1367-M1369.
18. J. Moncol, M. Mudra, P. Lonnecke, M. Koman, M. Melnik, *J. Chem. Crystallogr.* **2004**, *34*, 423–431.
19. D. P. Martone, A. W. Maverick, F. R. Fronczek, *Acta Crystallogr. C* **2007**, *63*, M238-M239.
20. L. J. Farrugia, *J. Appl. Crystallog.* **1997**, *30*, 565.
21. A. L. Spek, *J. Appl. Crystallogr.* **2003**, *36*, 7–13.
22. N. Lah, I. Leban, *Acta Crystallogr. E* **2005**, *61*, M1708–M1710.
23. K. D. Onan, M. Veidis, G. Davies, M. A. Elsayed, A. Eltoukhy, *Inorg. Chim. Acta* **1984**, *81*, 7–13.
24. W. E. Marsh, E. J. Valente, D. J. Hodgson, *Inorg. Chim. Acta* **1981**, *51*, 49–53.
25. D. O. Ivashkevich, A. S. Lyakhov, M. M. Degtyarik, P. N. Gaponik, *Acta Crystallogr. C* **2004**, *60*, M368–M370.
26. W. E. Estes, D. P. Gavel, W. E. Hatfield, D. J. Hodgson, *Inorg. Chem.* **1978**, *17*, 1415–1421.
27. B. Morosin, *Acta Crystallogr. B* **1975**, *B 31*, 632–634.
28. O. Castillo, A. Luque, S. Iglesias, P. Vitoria, P. Roman, *New J. Chem.* **2000**, *24*, 771–775.
29. O. Castillo, A. Luque, M. Julve, F. Lloret, P. Roman, *Inorg. Chim. Acta* **2001**, *315*, 9–17.

Povzetek

Dve vrsti bromidnih in kloridnih koordinacijskih spojin s 3-hidroksipiridinom (3-pyOH), $[CuX_2(3\text{-pyOH})_4]$ (**1**, **2**) tip A in $[Cu(\mu\text{-}X)_2(3\text{-pyOH})_2]_n$ (**3**, **4**) tip B (X = Br, Cl) sta bili pripravljeni. Kristalna struktura spojine $[CuBr_2(3\text{-pyOH})_4]$ **1** je bila določena z rentgensko strukturno analizo monokristalov. Le ta je pokazala oktaedrično koordinacijo okrog bakrovega(II) iona s štirimi dušikovimi atomi (3-pyOH) v ekvatorialni ravnini in dvema bromidnima anionoma na aksialnih mestih. Struktura tipa A kloridnega analoga $[CuCl_2(3\text{-pyOH})_4]$ **2** je bila določena z uporabo podatkov difrakcije prahu in monokristala. Molekulska struktura tipa B bromidnega kompleksa $[Cu(\mu\text{-}Br)_2(3\text{-pyOH})_2]_n$ **3** je bila določena s podatki difrakcije monokristala. V tej spojini so prisotne neskončno dolge ravne verige oblike *katena*-di-μ-bromidobis (3-pyOH)bakra(II). Primerjava podatkov rentgenske praškovne difrakcije spojin $[Cu(\mu\text{-}X)_2(3\text{-pyOH})_2]_n$ **3** in **4**, v povezavi z rezultati IR, UV-Vis ter magnetnimi metodami pokaže, da lahko uvrstimo obe spojini **3** in **4** v tip B, saj imata verjetno zelo podobno molekulsko strukturo. Magnetna susceptibilnost spojin tipa A enojedrnih kompleksov s konstantno $\chi_M \cdot T$ vrednostjo v območju 2–300 K prikazuje paramagnetno naravo spojin. Po drugi strani, širok vrh v krivulji $\chi_M(T)$ pod 50 K za večjedrne komplekse tipa B prikaže antiferomagnetno interakcijo med bakrovimi(II) $S = ½$ magnetnimi momenti. Ti podatki so bili primerjani z Bonner-Fischerjevo krivuljo (1D Heisenbergov antiferomagnet), ki pokaže J –17 cm^{-1} (**3**), –10 cm^{-1} (**4**). Opaženi paramagnetizem večjedrnih spojin **3**, **4** v EPR spektrih pri sobni temperaturi se sklada s spinom bakra(II), pri katerem je prisotno rombično popačenje spinskega tenzorja, ki je blizu aksialni simetriji.